

# Extreme Kuiper Belt Object 2001 QG<sub>298</sub> and the Fraction of Contact Binaries

Scott S. Sheppard and David Jewitt<sup>1</sup>

Institute for Astronomy, University of Hawaii,  
2680 Woodlawn Drive, Honolulu, HI 96822  
sheppard@ifa.hawaii.edu, jewitt@ifa.hawaii.edu

## ABSTRACT

Extensive time-resolved observations of Kuiper Belt object 2001 QG<sub>298</sub> show a lightcurve with a peak-to-peak variation of  $1.14 \pm 0.04$  magnitudes and single-peaked period of  $6.8872 \pm 0.0002$  hr. The mean absolute magnitude is 6.85 magnitudes which corresponds to a mean effective radius of 122 (77) km if an albedo of 0.04 (0.10) is assumed. This is the first known Kuiper Belt object and only the third minor planet with a radius  $> 25$  km to display a lightcurve with a range in excess of 1 magnitude. We find the colors to be typical for a Kuiper Belt object ( $B - V = 1.00 \pm 0.04$ ,  $V - R = 0.60 \pm 0.02$ ) with no variation in color between minimum and maximum light. The large light variation, relatively long double-peaked period and absence of rotational color change argue against explanations due to albedo markings or elongation due to high angular momentum. Instead, we suggest that 2001 QG<sub>298</sub> may be a very close or contact binary similar in structure to what has been independently proposed for the Trojan asteroid 624 Hektor. If so, its rotational period would be twice the lightcurve period or  $13.7744 \pm 0.0004$  hr. By correcting for the effects of projection, we estimate that the fraction of similar objects in the Kuiper Belt is at least  $\sim 10\%$  to  $20\%$  with the true fraction probably much higher. A high abundance of close and contact binaries is expected in some scenarios for the evolution of binary Kuiper Belt objects.

*Subject headings:* Kuiper Belt, Oort Cloud - minor planets, solar system: general

## 1. Introduction

The Kuiper Belt is a long-lived region of the Solar System just beyond Neptune where the planetisimals have not coalesced into a planet. It contains about 80,000 objects with radii greater than 50 km (Trujillo, Jewitt & Luu 2001) which have been collisionally processed and gravitationally perturbed throughout the age of the Solar System. The short-period comets and

---

<sup>1</sup>Visiting Astronomer, W.M. Keck Observatory, which operates as a scientific partnership among the California Institute of Technology, the University of California, and the National Aeronautics and Space Administration. The Observatory was made possible by the generous financial support of the W.M. Keck Foundation

Centaurs are believed to originate from the Kuiper Belt (Fernandez 1980; Duncan, Quinn & Tremaine 1988).

Physically, the Kuiper Belt objects (KBOs) show a large diversity of colors from slightly blue to ultra red ( $V - R \sim 0.3$  to  $V - R \sim 0.8$ , Luu and Jewitt 1996) and may show correlations between colors, inclination and/or perihelion distance (Jewitt & Luu 2001; Trujillo & Brown 2002; Doressoundiram et al. 2002; Tegler & Romanishin 2003). Spectra of KBOs are mostly featureless with a few showing hints of water ice (Brown, Cruikshank & Pendleton 1999; Jewitt & Luu 2001; Lazzarin et al. 2003). The range of KBO geometric albedos is still poorly sampled but the larger ones likely have values between 0.04 to 0.10 (Jewitt, Aussel & Evans 2001; Altenhoff, Bertoldi & Menten 2004). Time-resolved observations of KBOs show that  $\sim 32\%$  vary by  $\geq 0.15$  magnitudes,  $18\%$  by  $\geq 0.40$  magnitudes and  $12\%$  by  $\geq 0.60$  magnitudes (Sheppard & Jewitt 2002; Ortiz et al. 2003; Lacerda & Luu 2003; Sheppard & Jewitt 2004). One object, (20000) Varuna, displays a large photometric range and fast rotation which is best interpreted as a structurally weak object elongated by its own rotational angular momentum (Jewitt & Sheppard 2002). A significant fraction of KBOs appear to be more elongated than main-belt asteroids of similar size (Sheppard & Jewitt 2002). The KBO phase functions are steep, with a median of 0.16 magnitudes per degree between phase angles of 0 and 2 degrees (Sheppard & Jewitt 2002; Schaefer & Rabinowitz 2002; Sheppard & Jewitt 2004).

About  $4\% \pm 2\%$  of the KBOs are binaries with separations  $\geq 0.15''$  (Noll et al. 2002) while binaries with separations  $\geq 0.1''$  may constitute about 15% of the population (Trujillo 2003, private communication). All the binary KBOs found to date appear to have mass ratios near unity, though this may be an observational selection effect. The mechanism responsible for creating KBO binaries is not clear. Formation through collisions is unlikely (Stern 2002). Weidenschilling (2002) has proposed formation of such binaries through complex three-body interactions which would only occur efficiently in a much higher population of large KBOs than can currently be accounted for. Goldreich, Lithwick & Sari (2002) have proposed that KBO binaries could have formed when two bodies approach each other and energy is extracted either by dynamical friction from the surrounding sea of smaller KBOs or by a close third body. This process also requires that the density of KBOs was  $\sim 10^2$  to  $10^3$  times greater than now. They predict that closer binaries should be more abundant in the Kuiper Belt while Weidenschilling’s mechanism predicts the opposite.

The present paper is the fourth in a series resulting from the Hawaii Kuiper Belt variability project (HKBVP, see Jewitt & Sheppard 2002; Sheppard & Jewitt 2002; Sheppard & Jewitt 2004). The practical aim of the project is to determine the rotational characteristics (principally period and shape) of bright KBOs ( $m_R \leq 22$ ) in order to learn about the distributions of rotation period and shape in these objects. In the course of this survey we found that 2001 QG<sub>298</sub> had an extremely large light variation and a relatively long period. We have obtained optical observations of 2001 QG<sub>298</sub> in order to accurately determine the rotational lightcurve and constrain its possible causes. 2001 QG<sub>298</sub> has a typical Plutino orbit in 3:2 mean-motion resonance with Neptune,

semi-major axis at 39.2 AU, eccentricity of 0.19 and inclination of 6.5 degrees.

## 2. Observations

We used the University of Hawaii (UH) 2.2 m diameter telescope atop Mauna Kea in Hawaii to obtain R-band observations of 2001 QG<sub>298</sub> on three separate observing runs each covering several nights: UT September 12 and 13 2002; August 22, 26, 27 and 28 2003; September 27, 28 and 30 2003. Two different CCD cameras were employed. For the September 2002 and September 2003 observations we used a  $2048 \times 2048$  pixel Tektronix CCD ( $24 \mu\text{m}$  pixels) camera with a  $0.''219 \text{ pixel}^{-1}$  scale at the f/10 Cassegrain focus. An antireflection coating on the CCD gave very high average quantum efficiency (0.90) in the R-band. The field-of-view was  $7'.5 \times 7'.5$ . For the August 2003 observations we used the Orthogonal Parallel Transfer Imaging Camera (OPTIC). OPTIC has two  $4104 \times 2048$  pixel Lincoln Lab CCID28 Orthogonal Transfer CCDs developed to compensate for real-time image motion by moving the charge on the chips to compensate for seeing variations (Tonry, Burke & Schechter 1997). Howell et al. (2003) have demonstrated that these chips are photometrically accurate and provide routine sharpening of the image point spread function. There is a  $\sim 15''$  gap between the chips. The total field-of-view was  $9'.5 \times 9'.5$  with  $15 \mu\text{m}$  pixels which corresponds to  $0.14'' \text{ pixel}^{-1}$  scale at the f/10 Cassegrain focus. The same R-band filter based on the Johnson-Kron-Cousins photometric system was used for all UH 2.2 m observations.

In addition we used the Keck I 10 m telescope to obtain BVR colors of 2001 QG<sub>298</sub> at its maximum and minimum light on UT August 30, 2003. The LRIS camera with its Tektronix  $2048 \times 2048$  pixel CCD and  $24 \mu\text{m}$  pixels (image scale  $0.''215 \text{ pixel}^{-1}$ ) was used (Oke et al. 1995) with the facility broadband BVR filter set. Due to a technical problem with the blue camera side we used only the red side for photometry at BV and R. The blue filter response was cut by the use of a dichroic at  $0.460 \mu\text{m}$ .

All exposures were taken in a consistent manner with the telescope autoguided on bright nearby stars. The seeing ranged from  $0.''6$  to  $1.0''$  during the various observations. 2001 QG<sub>298</sub> moved relative to the fixed stars at a maximum of  $3''.5 \text{ hr}^{-1}$  corresponding to trail lengths  $\leq 0.''43$  in the longest (450 sec) exposures. Thus motion of the object was insignificant compared to the seeing.

Images from the UH telescope were bias-subtracted and then flat-fielded using the median of a set of dithered images of the twilight sky. Data from Keck were bias subtracted and flattened using flat fields obtained from an illuminated spot inside the closed dome. Landolt (1992) standard stars were employed for the absolute photometric calibration. To optimize the signal-to-noise ratio we performed aperture correction photometry by using a small aperture on 2001 QG<sub>298</sub> ( $0.''65$  to  $0.''88$  in radius) and both the same small aperture and a large aperture ( $2.''40$  to  $3.''29$  in radius) on (four or more) nearby bright field stars. We corrected the magnitude within the small aperture

used for the KBOs by determining the correction from the small to the large aperture using the field stars (c.f. Tegler and Romanishin 2000; Jewitt & Luu 2001; Sheppard & Jewitt 2002). Since 2001 QG<sub>298</sub> moved slowly we were able to use the same field stars from night to night within each observing run, resulting in very stable relative photometric calibration from night to night. The observational geometry for 2001 QG<sub>298</sub> on each night of observation is shown in Table 1.

### 3. Results

Tables 2 and 3 show the photometric results for 2001 QG<sub>298</sub>. We used the phase dispersion minimization (PDM) method (Stellingwerf 1978) to search for periodicity in the data. In PDM, the metric is the so-called  $\Theta$  parameter, which is essentially the variance of the unphased data divided by the variance of the data when phased by a given period. The best-fit period should have a very small dispersion compared to the unphased data and thus  $\Theta \ll 1$  indicates that a good fit has been found.

2001 QG<sub>298</sub> showed substantial variability ( $\sim 1.1$  magnitudes with a single-peaked period near 6.9 hr) in R-band observations from two nights in September 2002. We obtained further observations of the object in 2003 to determine the lightcurve with greater accuracy. PDM analysis of all the apparent magnitude R-band data from the September 2002 and August and September 2003 observations shows that 2001 QG<sub>298</sub> has strong  $\Theta$  minima near the periods  $P = 6.88$  hr and  $P = 13.77$  hr, with weaker alias periods flanking these (Figure 1). We corrected the apparent magnitude data for the minor phase angle effects (we used the nominal 0.16 magnitudes per degree found in Sheppard & Jewitt 2003) and light travel-time differences of the observations to correspond to the August 30, 2003 observations. We then phased the data to all the peaks with  $\Theta < 0.4$  and found only the 6.8872 and 13.7744 hour periods to be consistent with all the data (Figures 2 and 3). Through a closer look at the PDM plot (Figure 4) and phasing the data we find best fit periods  $P = 6.8872 \pm 0.0002$  hr (a lightcurve with a single maximum per period) and  $P = 13.7744 \pm 0.0004$  hr (two maxima per period as expected for rotational modulation caused by an aspherical shape). The double-peaked lightcurve appears to be the best fit with the minima different by about 0.1 magnitudes while the maxima appear to be of similar brightness. The photometric range of the lightcurve is  $\Delta m = 1.14 \pm 0.04$  magnitudes.

The Keck BVR colors of 2001 QG<sub>298</sub> show no variation from minimum to maximum light within the photometric uncertainties of a few % (see Figures 2 and 3). This is again consistent with a lightcurve that is produced by an elongated shape, rather than by albedo variations. The colors ( $B - V = 1.00 \pm 0.04$ ,  $V - R = 0.60 \pm 0.02$ ) show that 2001 QG<sub>298</sub> is red and similar to the mean values ( $B - V = 0.98 \pm 0.04$ ,  $V - R = 0.61 \pm 0.02$ , 28 objects) for KBOs as a group (Jewitt and Luu 2001).

The absolute magnitude of a Solar System object,  $m_R(1, 1, 0)$ , is the hypothetical magnitude the object would have if it were at heliocentric ( $R$ ) and geocentric ( $\Delta$ ) distances of 1 AU and

had a phase angle ( $\alpha$ ) of 0 degrees. We use the relation  $m_R(1, 1, 0) = m_R - 5\log(R\Delta) - \beta\alpha$  to find the absolute magnitude by correcting for the geometrical and phase angle effects in the 2001 QG<sub>298</sub> observations. Here  $m_R$  is the apparent red magnitude of the object and  $\beta$  is the phase function. Using the nominal value of  $\beta = 0.16$  magnitudes per degree for KBOs at low phase angles (Sheppard & Jewitt 2002; Sheppard & Jewitt 2004) and data from Table 1 we find that 2001 QG<sub>298</sub> has  $m_R(1, 1, 0) = 6.28 \pm 0.02$  at maximum light and  $m_R(1, 1, 0) = 7.42 \pm 0.02$  magnitudes at minimum light. If attributed to a rotational variation of the cross-section, this corresponds to a ratio of maximum to minimum areas of 2.85:1.

The effective radius of an object can be calculated using the relation  $m_R(1, 1, 0) = m_\odot - 2.5\log [p_R r_e^2 / 2.25 \times 10^{16}]$  where  $m_\odot$  is the apparent red magnitude of the sun ( $-27.1$ ),  $p_R$  is the red geometric albedo and  $r_e$  (km) is the effective circular radius of the object. If we assume an albedo of 0.04 (0.10) this corresponds to effective circular radii at maximum and minimum light of about 158 (100) km and 94 (59) km, respectively. At the mean absolute magnitude of 6.85 mag, the effective circular radius is 122 (77) km.

## 4. Analysis

Only three other objects in the Solar System larger than 25 km in radius are known to have lightcurve ranges  $> 1.0$  magnitude (Table 4). Following Jewitt and Sheppard (2002) we discuss three possible models of rotational variation to try to compare the objects from Table 4 with 2001 QG<sub>298</sub>.

### 4.1. Albedo Variation

On asteroids, albedo variations contribute brightness variations that are usually less than about 10% – 20% (Degewij, Tedesco & Zellner 1979). Rotationally correlated color variations may be seen if the albedo variations are large since materials with markedly different albedos may differ compositionally. As seen in Table 4, Saturn’s satellite Iapetus is the only object in which variations  $\geq 1$  mag. are explained through albedo. The large albedo contrast on Iapetus is likely a special consequence of its synchronous rotation and the anisotropic impact of material trapped in orbit about Saturn onto its leading hemisphere (Cook & Franklin 1970). Iapetus shows clear rotational color variations ( $\Delta(B - V) \sim 0.1$  mag.) that are correlated with the rotational albedo variations (Millis 1977) and which would be detected in 2001 QG<sub>298</sub> given the quality of our data. The special circumstance of Iapetus is without obvious analogy in the Kuiper Belt and we do not believe that it is a good model for the extreme lightcurve of 2001 QG<sub>298</sub>.

Pluto shows a much smaller variation (about 0.3 magnitudes) thought to be caused by albedo structure (Buie, Tholen & Wasserman 1997). Pluto is so large that it can sustain an atmosphere which may contribute to amplifying its lightcurve range by allowing surface frosts to condense on

brighter (cooler) spots. Thus brighter spots grow brighter while darker (hotter) spots grow darker through the sublimation of ices. This positive feedback mechanism requires an atmosphere and is unlikely to be relevant on a KBO as small as 2001 QG<sub>298</sub>.

While we cannot absolutely exclude surface markings as the dominant cause of 2001 QG<sub>298</sub>’s large rotational brightness variation, we are highly skeptical of this explanation. We measure no color variation with rotation, there appear to be two distinct minima and the range is so large as to be beyond reasonable explanation from albedo alone.

## 4.2. Aspherical Shape

Since surface markings are most likely not the cause of the lightcurve, the observed photometric variations are probably caused by changes in the projected cross-section of an elongated body in rotation about its minor axis. The rotation period of an elongated object should be twice the single-peaked lightcurve period because of the projection of both long axes (2 maxima) and short axes (2 minima) during one full rotation. If the body is elongated, we can use the ratio of maximum to minimum brightness to determine the projection of the body shape into the plane of the sky. The rotational brightness range of a triaxial object with semiaxes  $a \geq b \geq c$  in rotation about the  $c$  axis and viewed equatorially is

$$\Delta m = 2.5 \log \left( \frac{a}{b} \right) \quad (1)$$

where  $\Delta m$  is expressed in magnitudes. This gives a lower limit to  $a/b$  because of the effects of projection. Using  $\Delta m = 1.14$  for 2001 QG<sub>298</sub>, we find the lower limit is  $a/b = 2.85$ . This corresponds to  $a = 267$  and  $b = 94$  km for the geometric albedo 0.04 case and  $a = 169$  and  $b = 59$  km for an albedo of 0.10.

It is possible that 2001 QG<sub>298</sub> is elongated and able to resist gravitational compression into a spherical shape by virtue of its intrinsic compressive strength. However, observations of asteroids in the main-belt suggest that only the smallest ( $\sim 0.1$  km sized) asteroids are in possession of a tensile strength sufficient to resist rotational deformation (Pravec, Harris & Michalowski 2003). Observations of both asteroids and planetary satellites suggest that many objects with radii  $\geq 50$  to 75 km have shapes controlled by self-gravity, not by material strength (Farinella 1987; Farinella & Zappala 1997). The widely accepted explanation is that these bodies are internally weak because they have been fractured by numerous past impacts. This explanation is also plausible in the Kuiper Belt, where models attest to a harsh collisional environment at early times (e.g. Davis & Farinella 1997). We feel that the extraordinarily large amplitude of 2001 QG<sub>298</sub> is unlikely to be caused by elongation of the object sustained by its own material strength, although we cannot rule out this possibility.

Structurally weak bodies are susceptible to rotational deformation. The 1000-km scale KBO

(20000) Varuna (rotation period  $6.3442 \pm 0.0002$  hr and lightcurve range  $0.42 \pm 0.02$  mag) is the best current example in the Kuiper Belt (Jewitt and Sheppard 2002). In the main asteroid belt, 216 Kleopatra has a very short period (5.385 hr) and large lightcurve range (1.18 mag., corresponding to axis ratio  $\sim 2.95:1$  and dimensions  $\sim 217 \times 94$  km, Table 4). Kleopatra has been observed to be a highly elongated body through radar and high resolution imaging and the most likely explanation is that 216 Kleopatra is rotationally deformed (Leone et al. 1984; Ostro et al. 2000; Hestroffer et al. 2002; Washabaugh & Scheeres 2002). Is rotational elongation a viable model for 2001 QG<sub>298</sub>?

The critical rotation period ( $T_{crit}$ ) at which centripetal acceleration equals gravitational acceleration towards the center of a rotating spherical object is

$$T_{crit} = \left( \frac{3\pi}{G\rho} \right)^{1/2} \quad (2)$$

where  $G$  is the gravitational constant and  $\rho$  is the density of the object. With  $\rho = 1000$  kg m<sup>-3</sup> the critical period is about 3.3 hr. Even at longer periods, real bodies will suffer centripetal deformation into triaxial aspherical shapes which depend on their density, angular momentum and material strength. The limiting equilibrium shapes of rotating strengthless fluid bodies have been well studied by Chandrasekhar (1987) and a detailed discussion in the context of the KBOs can be found in Jewitt and Sheppard (2002). We briefly mention here that triaxial "Jacobi" ellipsoids with large angular momenta are rotationally elongated and generate lightcurves with substantial ranges when viewed equatorially.

Leone et al. (1984) have analyzed rotational equilibrium configurations of strengthless asteroids in detail (see Figure 5). They show that the maximum photometric range of a rotational ellipsoid is 0.9 mag: more elongated objects are unstable to rotational fission. The 1.14 mag photometric range of 2001 QG<sub>298</sub> exceeds this limit. In addition, the 13.7744 hr (two-peaked) rotation period is much too long to cause significant elongation for any plausible bulk density (Figure 5). For these reasons we do not believe that 2001 QG<sub>298</sub> is a single rotationally distorted object.

### 4.3. Binary Configurations

A third possible explanation for the extreme lightcurve of 2001 QG<sub>298</sub> is that this is an eclipsing binary. A wide separation (sum of the orbital semi-major axes much larger than the sum of the component radii) is unlikely because such a system would generate a distinctive "notched" lightcurve that is unlike the lightcurve of 2001 QG<sub>298</sub>. In addition, a wide separation would require unreasonably high bulk density of the components in order to generate the measured rotational period. If 2001 QG<sub>298</sub> is a binary then the components must be close or in contact. We next consider the limiting case of a contact binary.

The axis ratio of a contact binary consisting of equal spheres is  $a/b = 2$ , corresponding to a lightcurve range  $\Delta m = 0.75$  magnitudes, as seen from the rotational equator. At the average viewing angle  $\theta = 60$  degrees we would expect  $\Delta m = 0.45$  mag. The rotational variation of 2001 QG<sub>298</sub> is too large to be explained as a contact binary consisting of two equal spheres. However, close binary components of low strength should be elongated by mutual tidal forces, giving a larger lightcurve range than possible in the case of equal spheres (Leone et al. 1984). The latter authors find that the maximum range for a tidally distorted nearly contact binary is 1.2 magnitudes, compatible with the 1.14 mag. range of 2001 QG<sub>298</sub> (Figure 5). The contact binary hypothesis is the likely explanation of 624 Hektor’s lightcurve (Hartmann & Cruikshank 1978; Weidenschilling 1980; Leone et al. 1984) and could also explain 216 Kleopatra’s lightcurve (Leone et al. 1984; Ostro et al. 2000; Hestroffer et al. 2002).

We suggest that the relatively long double-peaked period ( $13.7744 \pm 0.0004$  hr) and large photometric range ( $1.14 \pm 0.04$  magnitudes) of 2001 QG<sub>298</sub>’s lightcurve are best understood if the body is a contact binary or nearly contact binary viewed from an approximately equatorial perspective. The large range suggests that the components are of similar size and are distorted by their mutual tidal interactions. Using the calculations from Leone et al. (1984), who take into account the mutual deformation of close, strengthless binary components, we find the density of these objects must be  $\sim 1000 \text{ kg m}^{-3}$  in order to remain bound in a binary system separated by the Roche radius (which is just over twice the component radius). If we assume that the albedo of both objects is 0.04, the effective radius of each component is about 95 km as found above. Using this information we find from Kepler’s third law that if the components are separated, they would be about 300 km apart. This separation as seen on the sky ( $0.01''$ ) is small enough to have escaped resolution with current technology.

Further, we point out that the maximum of the lightcurve of 2001 QG<sub>298</sub> is more nearly “U” shaped (or flattened) than is the “V” shaped minimum (Figure 3). This is also true for 624 Hektor (Dunlap & Gehrels 1969) and may be a distinguishing, though not unique, signature of a contact or nearly contact binary (Zappala 1984; Leone et al. 1984; Cellino et al. 1985). In comparison, (20000) Varuna, which is probably not a contact binary (see below and Jewitt & Sheppard 2002), does not show significant differences in the curvature of the lightcurve maxima and minima.

In short, while we cannot prove that 2001 QG<sub>298</sub> is a contact binary, we find by elimination of other possibilities that this is the most convincing explanation of its lightcurve.

#### 4.4. Fraction of Contact Binaries in the Kuiper Belt

The distribution of measured lightcurve properties is shown in Figure 5 (adapted from Figure 4 of Leone et al. (1984)). There, Region A corresponds to the low rotational range objects (of any period) in which the variability can be plausibly associated with surface albedo markings. Region B corresponds to the rotationally deformed Jacobi ellipsoids while Region



C marks the domain of the close binary objects. Plotted in the Figure are the lightcurve periods and ranges for KBOs from the HKBVP (Jewitt & Sheppard 2002; Sheppard & Jewitt 2002; Sheppard & Jewitt 2004). We also show large main belt asteroids (data from <http://cfa-www.harvard.edu/iau/lists/LightcurveDat.html> updated by A. Harris and B. Warner and based on Lagerkvist, Harris & Zappala 1989). Once again we note that the measured KBO ranges should, in most cases, be regarded as lower limits to the range because of the possible effects of projection into the plane of the sky.

Of the 34 KBOs in our sample, five fall into Region C in Figure 5. Of these, 2001 QG<sub>298</sub> is by far the best candidate for being a contact or nearly contact binary system since it alone has a range between the  $\Delta m_R \sim 0.9$  mag. limit for a single rotational equilibrium ellipsoid and the  $\Delta m_R \sim 1.2$  mag. limit for a mutually distorted close binary (Table 5). It is also rotating too slowly to be substantially distorted by its own spin (Figure 5). Both (33128) 1998 BU<sub>48</sub> and 2000 GN<sub>171</sub> are good candidates which have large photometric ranges and relatively slow periods. KBOs (26308) 1998 SM<sub>165</sub> and (32929) 1995 QY<sub>9</sub> could be rotationally deformed ellipsoids, but their relatively slow rotations would require densities much smaller than that of water, a prospect which we consider unlikely.

We next ask what might be the abundance of contact or close binaries in the Kuiper Belt. As a first estimate we assume that we have detected one such object (2001 QG<sub>298</sub>) in a sample of 34 KBOs observed with adequate time resolution. The answer depends on the magnitude of the correction for projection effects caused by the orientation of the rotation vector with respect to the line of sight. This correction is intrinsically uncertain, since it depends on unknowns such as the scattering function of the surface materials of the KBO as well as on the detailed shape. We adopt two crude approximations that should give the projection correction at least to within a factor of a few.

First, we represent the elongated shape of the KBO by a rectangular block with dimensions  $a > b = c$ . The lightcurve range varies with angle from the equator,  $\theta$ , in this approximation as

$$\Delta m = 2.5 \log \left[ \frac{1 + \tan \theta}{\frac{b}{a} + \tan \theta} \right]. \quad (3)$$

For the limiting case of a highly distorted contact binary with  $\Delta m = 1.2$  mag. at  $\theta = 0^\circ$ , Eq. (3) gives  $a/b = 3$ . We next assume that the range must fall in the range  $0.9 \leq \Delta m \leq 1.2$  mag. in order for us to make an assignment of likely binary structure (Figure 6). As noted above, only 2001 QG<sub>298</sub> satisfies this condition amongst the known objects. We find, from Eq. (3) with  $a/b = 3$ , that  $\Delta m = 0.9$  mag is reached at  $\theta = 10^\circ$ . The probability that Earth would lie within  $10^\circ$  of the equator of a set of randomly oriented KBOs is  $P(\theta \leq 10) = 0.17$ . Therefore, the detection of 1 KBO with  $0.9 \leq \Delta m \leq 1.2$  mag implies that the fractional abundance of similarly elongated objects is  $f \sim 1/(34P) \sim 17\%$ .

As a separate check on this estimate, we next represent the object as an ellipsoid, again with

axes  $a > b = c$ . The photometric range when viewed at an angle  $\theta$  from the rotational equator is given by

$$\Delta m = 2.5 \log(a/b) - 1.25 \log \left[ \left[ \left( \frac{a}{b} \right)^2 - 1 \right] \sin^2 \theta + 1 \right] \quad (4)$$

Substituting  $a/b = 3$ , the range predicted by Eq. (4) falls to 0.9 mag at  $\theta \sim 17^\circ$ . Given a random distribution of the spin vectors, the probability that Earth would lie within  $17^\circ$  of the equator is  $P(\theta \leq 17) = 0.29$ . Therefore, the detection of 1 KBO with a range between 0.9 and 1.2 mag in a sample of 34 objects implies, in this approximation, a fractional abundance of similarly elongated objects near  $f \sim 1/(34P) \sim 10\%$ .

Given the crudity of the model, the agreement between projection factors from Eqs. (3) and (4) is encouraging. Together, the data and the projection factors suggest that in our sample of 34 KBOs, perhaps 3 to 6 objects are as elongated as 2001 QG<sub>298</sub> but only 2001 QG<sub>298</sub> is viewed from a sufficiently equatorial perspective that the lightcurve is distinct. This is consistent with Figure 5, which shows that 5 of 34 KBOs (15%) from the HKBVP occupy Region C of the period-range diagram. Our estimate is very crude and is also a lower limit to the true binary fraction because close binaries with components of unequal size will not satisfy the  $0.9 \leq \Delta m \leq 1.2$  mag. criterion for detection. The key point is that the data are consistent with a substantial close binary fraction in the Kuiper Belt .

Figure 5 also shows that there are no large main-belt asteroids (radii  $\geq 100$  km) in Region C, which is where similar sized component contact binaries are expected to be. To date, no examples of large binary main-belt asteroids with similar sized components have been found, even though the main belt has been extensively searched for binarity (see Margot 2002 and references therein). The main-belt asteroids may have had a collisional history significantly different from that of the KBOs.

The contact binary interpretation of the 2001 QG<sub>298</sub> lightcurve is clearly non-unique. Indeed, firm proof of the existence of contact binaries will be as difficult to establish in the Kuiper Belt as it has been in closer, brighter populations of small bodies. Nevertheless, the data are compatible with a high abundance of such objects. It is interesting to speculate about how such objects could form in abundance. One model of the formation and long term evolution of wide binaries predicts that such objects could be driven together by dynamical friction or three-body interactions (Goldreich et al. 2002). Objects like 2001 QG<sub>298</sub> would be naturally produced by such a mechanism.

## 5. Summary

Kuiper Belt Object 2001 QG<sub>298</sub> has the most extreme lightcurve of any of the 34 objects so far observed in the Hawaii Kuiper Belt Variability Project.

1. The double-peaked lightcurve period is  $13.7744 \pm 0.0004$  hr and peak-to-peak range is  $1.14 \pm 0.04$  mag. Only two other minor planets with radii  $\geq 25$  km (624 Hektor and 216 Kleopatra) and one planetary satellite (Iapetus) are known to show rotational photometric variation greater than 1 mag.
2. The absolute red magnitude is  $m_R(1,1,0) = 6.28$  at maximum light and 7.42 mag. at minimum light. With an assumed geometric albedo of 0.04 (0.10) we derive effective circular radii at maximum and minimum light of 158 (100) and 94 (59) km, respectively.
3. No variation in the BVR colors between maximum and minimum light was detected to within photometric uncertainties of a few percent.
4. The large photometric range, differences in the lightcurve minima, and long period of 2001 QG<sub>298</sub> are consistent with and strongly suggest that this object is a contact or nearly contact binary, viewed equatorially.
5. If 2001 QG<sub>298</sub> is a contact binary with similarly sized components, then we conclude that such objects constitute at least 10% to 20% of the Kuiper Belt population at large sizes.

## Acknowledgments

We thank John Tonry and Andrew Pickles for help with the OPTIC camera and the remote observing system on the University of Hawaii 2.2 meter telescope. We also thank Henry Hsieh for observational assistance and Jane Luu for comments on the manuscript. This work was supported by a grant to D.J. from the NASA Origins Program.

## REFERENCES

- Altenhoff, W., Bertoldi, F. & Menten, K. 2004, AA, in press
- Binzel, R. & Sauter, L. 1992, Icarus, 95, 222
- Brown, R., Cruikshank, D. & Pendleton, Y. 1999, ApJ, 519L, 101
- Buie, M., Tholen, D. & Wasserman, L. 1997, Icarus, 125, 233
- Cellino, A., Pannunzio, R., Zappala, V., Farinella, P. & Paolicchi, P. 1985, A&A, 144, 355
- Chandrasekhar, S. 1987, Ellipsoidal Figures of Equilibrium. Dover, New York.
- Cook, A. & Franklin, F. 1970, Icarus, 13, 282

- Davis, D. & Farinella, P. 1997, *Icarus*, 125, 50
- Degewij, J., Tedesco, E., & Zellner, B. 1979, *Icarus*, 40, 364
- Doressoundiram, A., Peixinho, N., de Bergh, C., Fornasier, S., Thebault, P., Barucci, M. & Veillet, C. 2003, *AJ*, 125, 1629
- Duncan, M., Quinn, T. & Tremaine, S. 1988, *ApJ*, 328, L69
- Dunlap, J. & Gehrels, T. 1969, *AJ*, 74, 796
- Farinella, P., Paolicchi, P., Tedesco, E., & Zappala, V. 1981, *Icarus*, 46, 114
- Farinella, P. 1987, in *The Evolution of the Small Bodies of the Solar System*, eds. M. Fulchignoni & L. Kresak (Amsterdam: North-Holland), 276
- Farinella, P. & Zappala, V. 1997, *Adv. Space Res.*, 19, 181
- Fernandez, J. 1980, *MNRAS*, 192, 481
- Goldreich, P., Lithwick, Y. & Sari, R. 2002, *Nature*, 420, 643
- Hartmann, W. & Cruikshank, D. 1978, *Icarus*, 36, 353
- Hartmann, W., Tholen, D., Goguen, J., Binzel, R. & Cruikshank, D. 1988, *Icarus*, 73, 487
- Hestroffer, D., Marchis, F., Fusco, T. & Berthier, J. 2002, *A&A*, 394, 339
- Howell, S., Everett, M., Tonry, J., Pickles, A. & Dain, C. 2003, *PASP*, 115, 1340
- Jewitt, D. & Luu, J. 2001, *AJ*, 122, 2099
- Jewitt, D., Aussel, H. & Evans, A. 2001, *Nature*, 411, 446
- Jewitt, D. & Sheppard, S. 2002, *AJ*, 123, 2110
- Lacerda, P. & Luu, J. 2003, *Icarus*, 161, 174
- Lagerkvist, C., Harris, A. & Zappala, V. 1989, in *Asteroids II*, ed. R. Binzel, T. Gehrels, and M. Matthews (Tucson: Univ. of Arizona Press), 1162
- Landolt, A. 1992, *AJ*, 104, 340
- Lazzarin, M., Barucci, M., Boehnhardt, H., Tozzi, G., de Bergh, C. & Dotto, E. 2003, *AJ*, 125, 1554
- Leone, G., Farinella, P., Paolicchi, P. & Zappala, V. 1984, *A&A*, 140, 265
- Luu, J. & Jewitt, D. 1996, *AJ*, 112, 2310
- Margot, J. 2002, *Nature*, 416, 694
- Merline, W. et al. 2001, *IAU Circular*, 7741
- Millis, R. 1977, *Icarus*, 31, 81
- Noll, K., Stephens, D., Grundy, W., Millis, R., Spencer, J., Buie, M., Tegler, S., Romanishin, W. & Cruikshank, D. 2002, *AJ*, 124, 3424
- Oke, J. et al. 1995, *PASP*, 107, 375

- Ortiz, J., Gutierrez, P., Casanova, V. & Sota, A. 2003, AA, 407, 1149
- Ostro, S., et al. 2000, Science, 288, 836
- Pravec, P., Harris, A. & Michalowski, T. 2003, in Asteroids III, eds. W. Bottke, A. Cellino, P. Paolicchi & R. Binzel (Tucson: Univ. of Arizona Press), 113
- Romanishin, W., Tegler, S., Rettig, T., Consolmagno, G., & Botthof, B. 2001, Proc. Nat. Academy Sci., 98, 11863
- Scaltriti, F. & Zappala, V. 1978, Icarus 34, 428
- Schaefer, B. & Rabinowitz, D. 2002, Icarus, 160, 52
- Sheppard, S. & Jewitt, D. 2002, AJ, 124, 1757
- Sheppard, S. & Jewitt, D. 2004, EM&P, in press
- Stellingwerf, R. 1978, ApJ, 224, 953
- Stern, A. 2002, AJ, 124, 2300
- Tegler, S. & Romanishin, W. 2003 Icarus, 161, 181
- Tegler, S. & Romanishin, W. 2000, Nature, 407, 979
- Tholen, D. 1980, S&T, 60, 203
- Tonry, J., Burke, B. & Schechter, P. 1997, PASP, 109, 1154
- Trujillo, C., Jewitt, D. & Luu, J. 2001, AJ, 122, 457
- Trujillo, C. & Brown, M. 2002, ApJ, 566, 125
- Washabaugh, P. & Scheeres, D. 2002, Icarus, 159, 314
- Weidenschilling, S. 1980, Icarus, 44, 807
- Weidenschilling, S. 2002, Icarus, 160, 212
- Zappala, V. 1980, The Moon and Planets, 23, 345

Fig. 1.— The phase dispersion minimization (PDM) plot for 2001 QG<sub>298</sub>. A smaller theta corresponds to a better fit. Best fits from this plot are the 6.8872 hour single-peaked fit and the 13.7744 hour double-peaked fit. Both are flanked by alias periods.

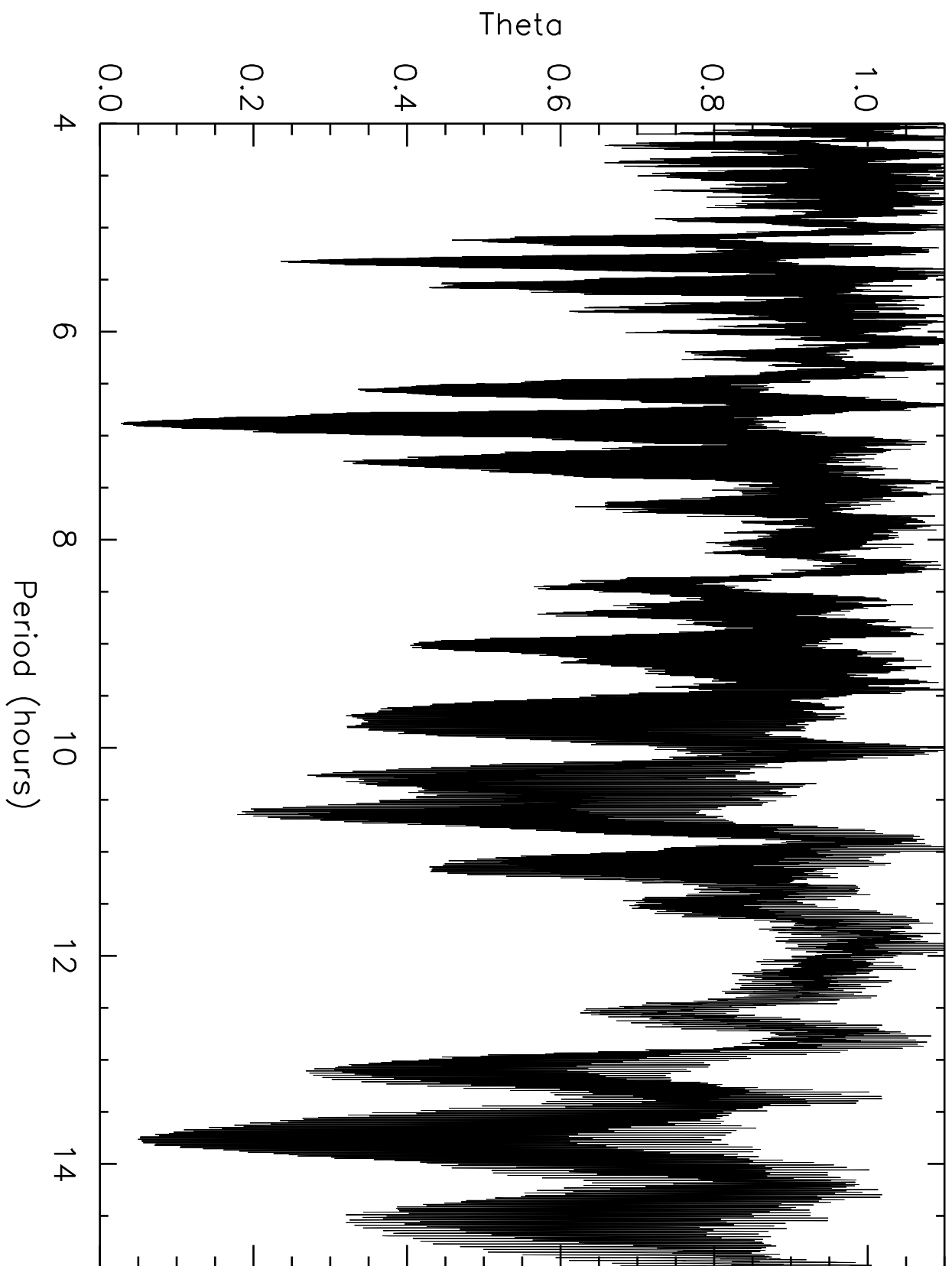
Fig. 2.— Phased data from all the observations in 2002 and 2003 of 2001 QG<sub>298</sub>. The period has been phased to 6.8872 hr which is the best fit single-peaked period. Filled colored symbols are data taken in the B-band (blue), V-band (green) and R-band (red) at the Keck I telescope on UT August 30. All other symbols are R-band data from the various nights of observations at UH 2.2 m telescope. The *B* and *V* points have been shifted according to their color differences from the R-band ( $V - R = 0.60$  and  $B - V = 1.00$ ). No color variation is seen between maximum and minimum light. The uncertainty on each photometric observation is  $\pm 0.03$  mag.

Fig. 3.— Phased data from all the observations in 2002 and 2003 of 2001 QG<sub>298</sub>. The period has been phased to 13.7744 hr which is the best fit double-peaked period. Filled colored symbols are data taken in the B-band (blue), V-band (green) and R-band (red) at the Keck I telescope on UT August 30. All other symbols are R-band data from the various nights of observations at UH 2.2 m telescope. The *B* and *V* points have been shifted according to their color differences from the R-band ( $V - R = 0.60$  and  $B - V = 1.00$ ). There appears to be two distinct minima. The minima appear to be more “notched” compared to the flatter maxima. No color variation is seen between maximum and minimum light. The uncertainty for each photometric observation is  $\pm 0.03$  mag.

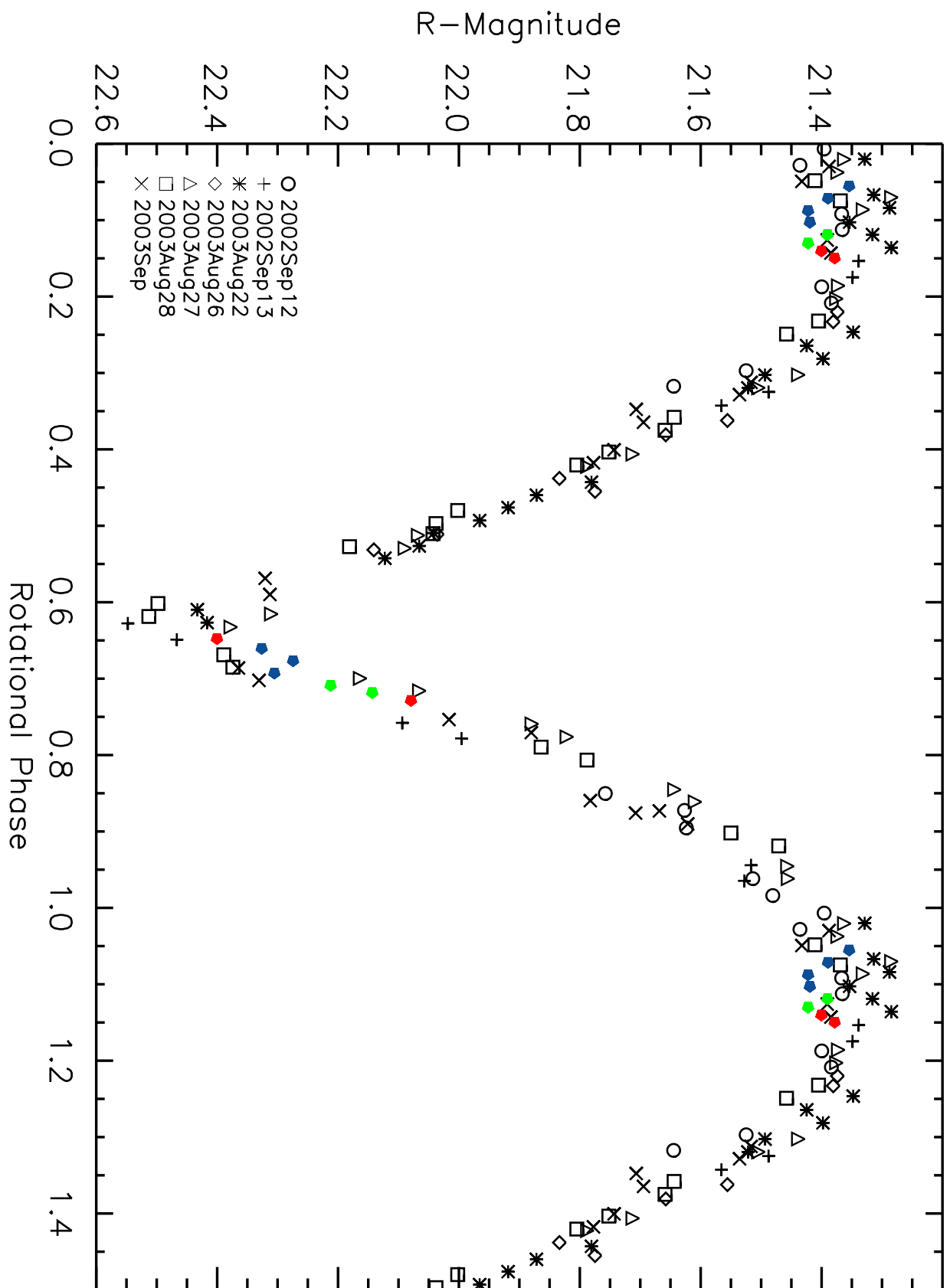
Fig. 4.— A closer view of the phase dispersion minimization (PDM) plot for 2001 QG<sub>298</sub> around the double-peaked period at 13.7744 hr. The best fit is flanked by aliases from separation of the 3 data sets obtained for this object. Only the center PDM peak fits the data once it is phased together.

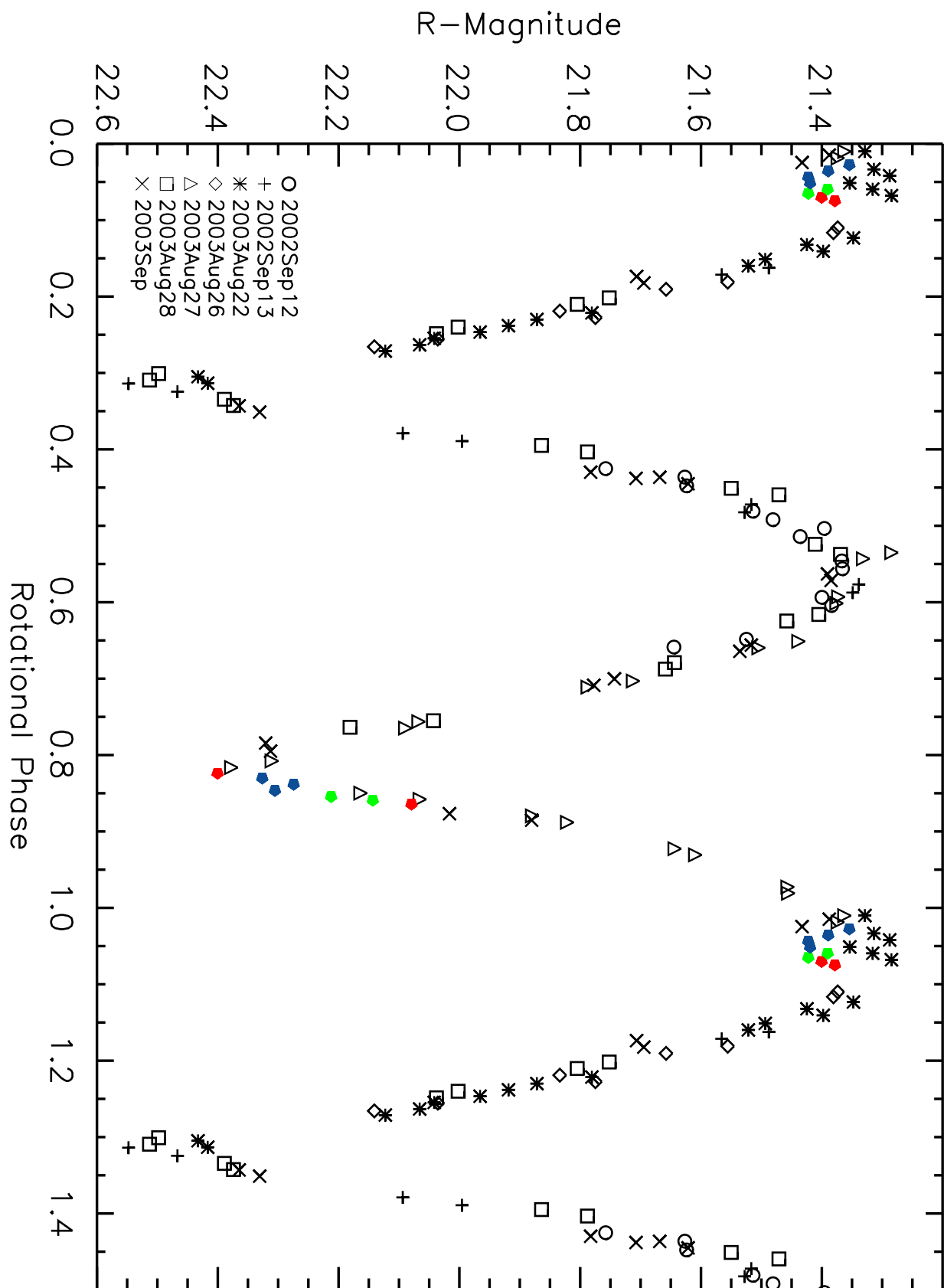
Fig. 5.— This Figure is a modification of Figure 4 from Leone et al. (1984). We here show the rotation periods and photometric ranges of known KBO lightcurves and the larger asteroids. The Regions are defined as A) The range of the lightcurve could be equally caused by albedo, elongation or binarity B) The lightcurve range is most likely caused by rotational elongation C) The lightcurve range is most likely caused by binarity of the object. Stars denote KBOs, Circles denote main-belt asteroids (radii  $\geq 100$  km) and Squares denote the Trojan 624 Hektor and the main-belt asteroid 216 Kleopatra. Objects just to the left of Region B would have densities significantly less than  $1000 \text{ kg m}^{-3}$  in order to be elongated from rotational angular momentum. Binary objects are not expected to have photometric ranges above 1.2 magnitudes. The 23 KBOs which have photometric ranges below our photometric uncertainties ( $\sim 0.1$  mag) in our Hawaii survey have not been plotted since their periods are unknown. These objects would all fall into Region A. The asteroids have been plotted at their expected mean projected viewing angle of 60 degrees in order to more directly compare to the KBOs of unknown projection angle.

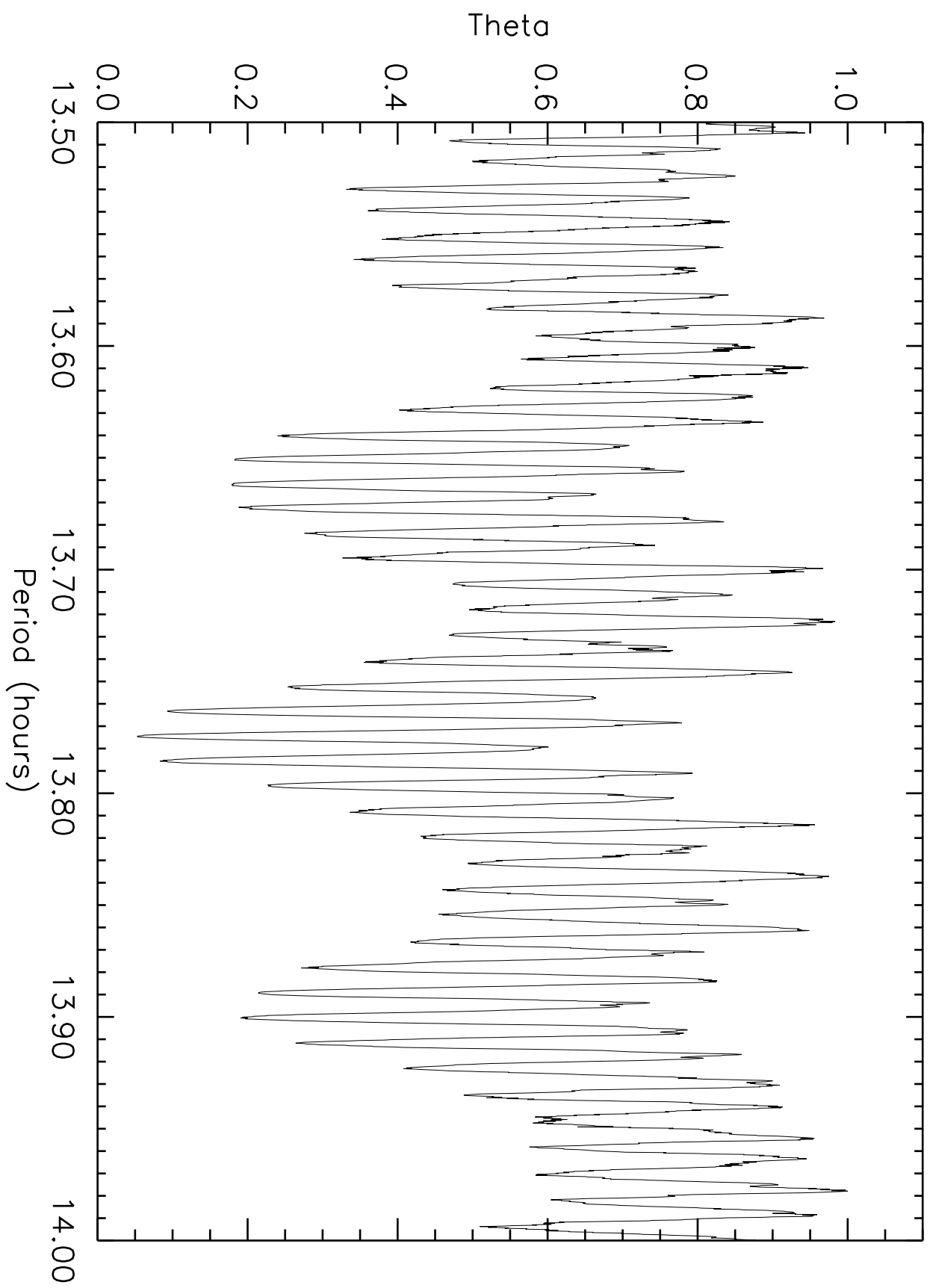
Fig. 6.— A histogram of known KBOs photometric ranges. There is a break in known photometric ranges starting around 0.25 magnitudes. The Regions are defined as 1) The lightcurve range could be dominated by albedo, elongation or binarity 2) The lightcurve is likely dominated from rotational elongation or binarity 3) The lightcurve is likely caused by binarity. Data is from our Hawaii Kuiper Belt object variability project (Sheppard & Jewitt 2002 and Sheppard and Jewitt 2004).

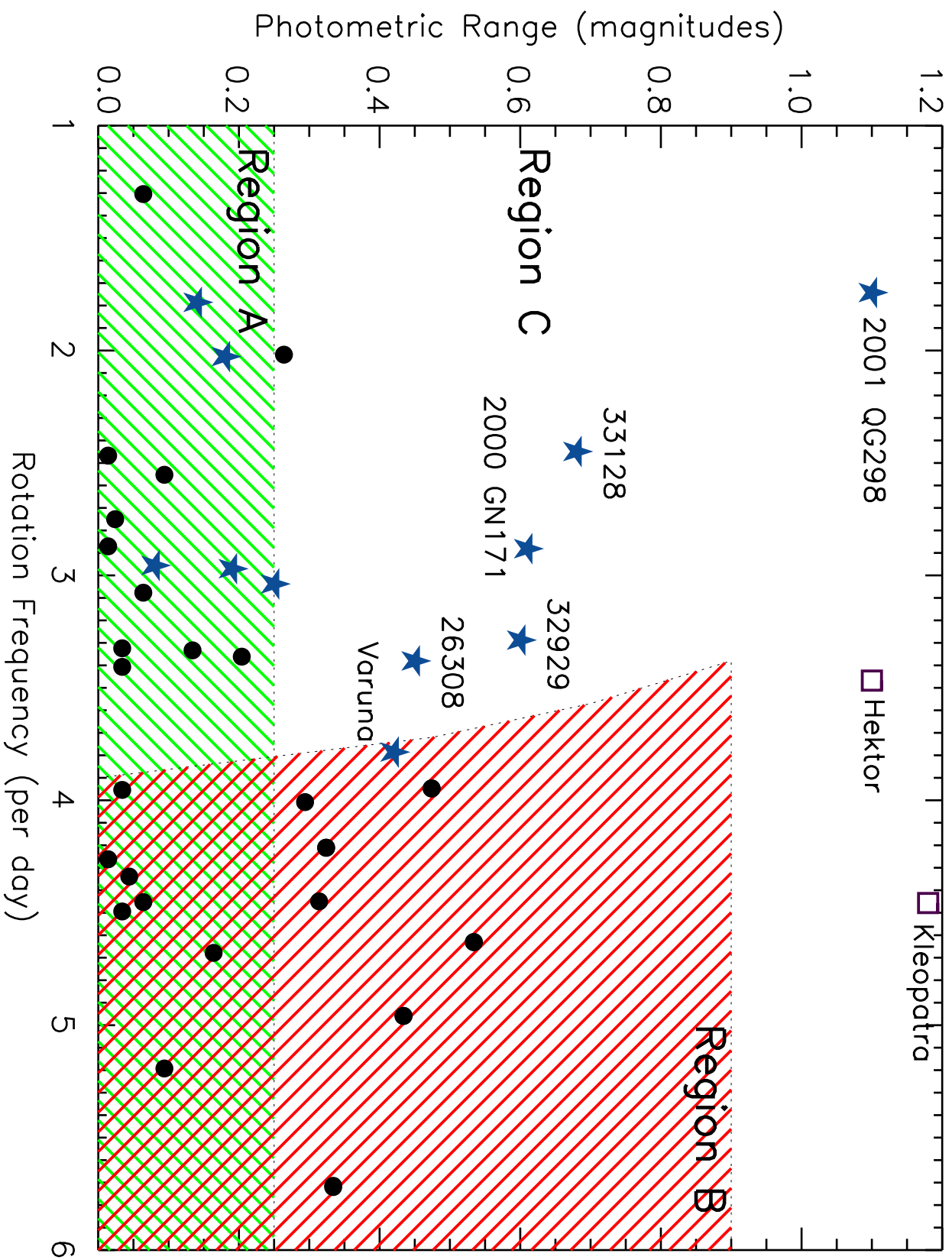












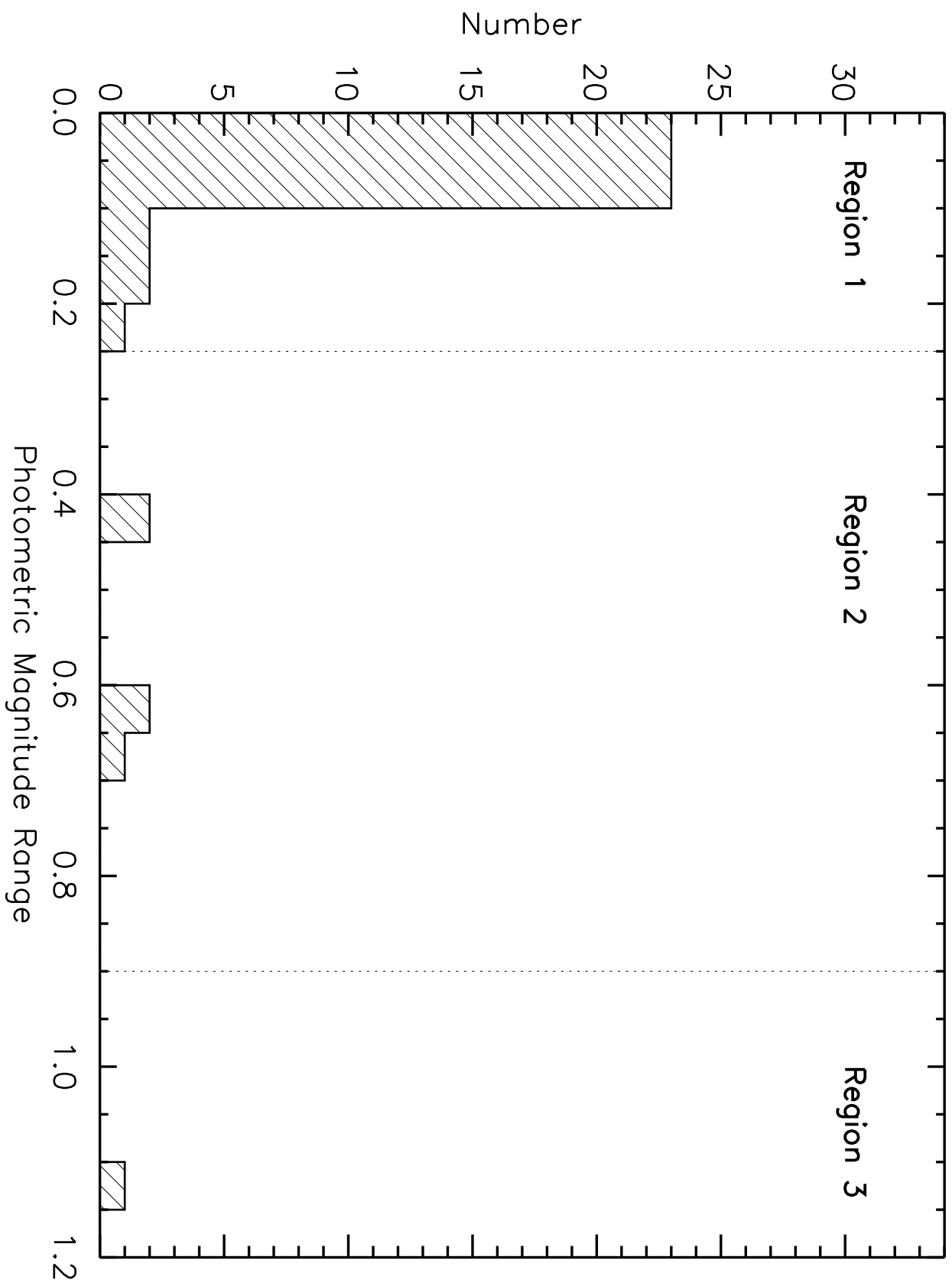


TABLE 1. Geometrical Circumstances of the Observations

UT Date	R (AU)	$\Delta$ (AU)	$\alpha$ (deg)
2002 Sep 12	32.0028	30.9994	0.151
2002 Sep 13	32.0026	30.9983	0.119
2003 Aug 22	31.9392	31.0405	0.851
2003 Aug 26	31.9385	31.0112	0.738
2003 Aug 27	31.9384	31.0046	0.709
2003 Aug 28	31.9382	30.9982	0.680
2003 Aug 30	31.9378	30.9863	0.622
2003 Sep 27	31.9330	30.9407	0.253
2003 Sep 28	31.9328	30.9434	0.283
2003 Sep 30	31.9325	30.9497	0.345

TABLE 2. R-band Observations at the UH 2.2 meter telescope

Image <sup>a</sup>	UT Date <sup>b</sup>	Julian Date <sup>c</sup>	Exp <sup>d</sup> (sec)	Mag. <sup>e</sup> ( $m_R$ )
nt3023	2002 Sep 12.32535	2452529.825347	450	21.673
nt3024	2002 Sep 12.33185	2452529.831840	450	21.542
nt3025	2002 Sep 12.33836	2452529.838356	450	21.539
nt3028	2002 Sep 12.35733	2452529.857326	450	21.429
nt3029	2002 Sep 12.36383	2452529.863819	450	21.396
nt3030	2002 Sep 12.37045	2452529.870451	400	21.311
nt3031	2002 Sep 12.37646	2452529.876458	400	21.351
nt3034	2002 Sep 12.39474	2452529.894734	400	21.282
nt3035	2002 Sep 12.40065	2452529.900648	400	21.281
nt3038	2002 Sep 12.42219	2452529.922188	400	21.315
nt3039	2002 Sep 12.42811	2452529.928102	400	21.299
nt3043	2002 Sep 12.45360	2452529.953600	400	21.440
nt3044	2002 Sep 12.45952	2452529.959514	400	21.560
nt4047	2002 Sep 13.32242	2452530.822419	350	21.398
nt4048	2002 Sep 13.32776	2452530.827755	350	21.476
nt4071	2002 Sep 13.40951	2452530.909514	400	22.458
nt4072	2002 Sep 13.41544	2452530.915428	400	22.377
nt4083	2002 Sep 13.44672	2452530.946725	400	22.004
nt4084	2002 Sep 13.45264	2452530.952639	400	21.906
nt4097	2002 Sep 13.50026	2452531.000255	400	21.427
nt4098	2002 Sep 13.50617	2452531.006169	400	21.438
nt4112	2002 Sep 13.56040	2452531.060394	400	21.249
nt4113	2002 Sep 13.56631	2452531.066308	400	21.259
f.114	2003 Aug 22.44983	2452873.949815	400	21.356
f.115	2003 Aug 22.46309	2452873.963079	400	21.341
f.116	2003 Aug 22.46815	2452873.968125	400	21.315
f.117	2003 Aug 22.47331	2452873.973287	380	21.381
f.118	2003 Aug 22.47812	2452873.978090	380	21.343
f.119	2003 Aug 22.48288	2452873.982859	380	21.312
f.124	2003 Aug 22.51473	2452874.014711	380	21.375
f.125	2003 Aug 22.51984	2452874.019815	380	21.452
f.126	2003 Aug 22.52467	2452874.024630	380	21.425
f.127	2003 Aug 22.53082	2452874.030799	380	21.521
f.128	2003 Aug 22.53559	2452874.035567	380	21.549
f.138	2003 Aug 22.57113	2452874.071111	380	21.808
f.139	2003 Aug 22.57589	2452874.075868	380	21.899
f.140	2003 Aug 22.58063	2452874.080613	380	21.946
f.141	2003 Aug 22.58543	2452874.085405	380	21.993
f.142	2003 Aug 22.59016	2452874.090150	380	22.069
f.143	2003 Aug 22.59494	2452874.094919	380	22.093
f.144	2003 Aug 22.59972	2452874.099699	380	22.150
f.147	2003 Aug 22.61900	2452874.118981	380	22.460
f.148	2003 Aug 22.62375	2452874.123738	380	22.444
nt1115	2003 Aug 26.52466	2452878.024653	300	21.383
nt1116	2003 Aug 26.52830	2452878.028287	300	21.390
nt1137	2003 Aug 26.56556	2452878.065544	400	21.565
nt1138	2003 Aug 26.57085	2452878.070833	400	21.667
nt1141	2003 Aug 26.58721	2452878.087187	400	21.843

TABLE 2. (continued)

Image <sup>a</sup>	UT Date <sup>b</sup>	Julian Date <sup>c</sup>	Exp <sup>d</sup> (sec)	Mag. <sup>e</sup> ( $m_R$ )
nt1142	2003 Aug 26.59203	2452878.092014	400	21.784
nt1145	2003 Aug 26.60817	2452878.108171	400	22.045
nt1146	2003 Aug 26.61414	2452878.114120	400	22.150
nt2057	2003 Aug 27.34245	2452878.842442	400	21.289
nt2058	2003 Aug 27.34729	2452878.847280	400	21.336
nt2068	2003 Aug 27.37572	2452878.875706	400	21.377
nt2069	2003 Aug 27.38053	2452878.880521	400	21.380
nt2072	2003 Aug 27.40915	2452878.909144	400	21.443
nt2073	2003 Aug 27.41403	2452878.914016	400	21.509
nt2080	2003 Aug 27.43887	2452878.938854	400	21.717
nt2081	2003 Aug 27.44368	2452878.943669	400	21.792
nt2090	2003 Aug 27.46950	2452878.969479	400	22.072
nt2091	2003 Aug 27.47431	2452878.974294	400	22.094
nt2098	2003 Aug 27.49900	2452878.998981	400	22.315
nt2099	2003 Aug 27.50382	2452879.003808	400	22.382
nt2104	2003 Aug 27.52311	2452879.023090	400	22.168
nt2105	2003 Aug 27.52795	2452879.027928	400	22.070
nt2108	2003 Aug 27.54033	2452879.040324	400	21.884
nt2109	2003 Aug 27.54516	2452879.045139	400	21.826
nt2114	2003 Aug 27.56485	2452879.064826	400	21.648
nt2115	2003 Aug 27.56971	2452879.069688	400	21.614
nt2122	2003 Aug 27.59367	2452879.093657	400	21.461
nt2123	2003 Aug 27.59849	2452879.098472	400	21.460
nt2127	2003 Aug 27.61524	2452879.115220	400	21.367
nt2128	2003 Aug 27.62006	2452879.120046	400	21.378
nt3062	2003 Aug 28.29908	2452879.799074	400	21.752
nt3063	2003 Aug 28.30389	2452879.803877	400	21.805
nt3066	2003 Aug 28.32106	2452879.821053	400	22.002
nt3067	2003 Aug 28.32587	2452879.825868	400	22.038
nt3079	2003 Aug 28.35605	2452879.856042	400	22.498
nt3080	2003 Aug 28.36082	2452879.860810	400	22.513
nt3083	2003 Aug 28.37516	2452879.875150	400	22.389
nt3084	2003 Aug 28.37992	2452879.879907	400	22.374
nt3093	2003 Aug 28.40996	2452879.909942	400	21.864
nt3094	2003 Aug 28.41477	2452879.914757	400	21.788
nt3108	2003 Aug 28.44225	2452879.942234	400	21.550
nt3109	2003 Aug 28.44701	2452879.946991	400	21.471
nt3132	2003 Aug 28.48418	2452879.984167	400	21.411
nt3133	2003 Aug 28.49170	2452879.991690	400	21.369
nt3164	2003 Aug 28.53695	2452880.036933	400	21.405
nt3165	2003 Aug 28.54172	2452880.041713	400	21.458
nt3187	2003 Aug 28.57313	2452880.073113	400	21.644
nt3188	2003 Aug 28.57790	2452880.077882	400	21.659
nt3215	2003 Aug 28.61676	2452880.116748	400	22.043
nt3216	2003 Aug 28.62153	2452880.121516	400	22.181
nt1.034	2003 Aug 27.27855	2452909.778553	300	21.600
nt1.035	2003 Aug 27.28337	2452909.783368	300	21.553
nt1.067	2003 Aug 27.42997	2452909.929965	300	21.675



TABLE 2. (continued)

Image <sup>a</sup>	UT Date <sup>b</sup>	Julian Date <sup>c</sup>	Exp <sup>d</sup> (sec)	Mag. <sup>e</sup> ( $m_R$ )
nt1.068	2003 Aug 27.43473	2452909.934734	300	21.709
nt1.089	2003 Aug 27.53125	2452910.031238	300	21.948
nt1.090	2003 Aug 27.53605	2452910.036042	300	21.812
nt2.032	2003 Aug 28.27564	2452910.775637	300	21.643
nt2.033	2003 Aug 28.28043	2452910.780428	300	21.631
nt2.053	2003 Aug 28.37271	2452910.872708	300	22.301
nt2.054	2003 Aug 28.37751	2452910.877512	300	22.267
nt2.063	2003 Aug 28.42250	2452910.922500	300	21.719
nt2.064	2003 Aug 28.42730	2452910.927292	300	21.644
nt2.080	2003 Aug 28.49909	2452910.999086	300	21.327
nt2.081	2003 Aug 28.50389	2452911.003889	300	21.321
nt2.090	2003 Aug 28.55245	2452911.052442	300	21.453
nt2.091	2003 Aug 28.55725	2452911.057245	300	21.472
nt2.166	2003 Aug 30.34785	2452912.847847	400	22.267
nt2.167	2003 Aug 30.35398	2452912.853981	400	22.259
nt2.195	2003 Aug 30.48012	2452912.980116	400	21.334
nt2.196	2003 Aug 30.48597	2452912.985961	400	21.379

<sup>a</sup>Image number.<sup>b</sup>Decimal Universal Date at the start of the integration.<sup>c</sup>Julian Date at the start of the integration. No light-time correction has been made in the table.<sup>d</sup>Exposure time for the image.<sup>e</sup>Apparent red magnitude, uncertainties are  $\pm 0.03$  to  $\pm 0.04$ .

TABLE 3. B-band, V-band and R-band Observations at Keck

Image <sup>a</sup>	UT Date <sup>b</sup>	Julian Date <sup>c</sup>	Exp <sup>d</sup> (sec)	Mag.
lred0078	2003 Aug 30.37786	2452881.877861	150	22.391 <sup>e</sup>
lred0084	2003 Aug 30.40107	2452881.901076	150	22.070 <sup>e</sup>
lred0120	2003 Aug 30.51921	2452882.019213	150	21.391 <sup>e</sup>
lred0121	2003 Aug 30.52202	2452882.022027	150	21.369 <sup>e</sup>
lred0082	2003 Aug 30.39546	2452881.895460	150	22.803 <sup>f</sup>
lred0083	2003 Aug 30.39828	2452881.898285	150	22.734 <sup>f</sup>
lred0118	2003 Aug 30.51329	2452882.013295	150	21.981 <sup>f</sup>
lred0119	2003 Aug 30.51642	2452882.016423	150	22.013 <sup>f</sup>
lred0079	2003 Aug 30.38170	2452881.881700	300	23.917 <sup>g</sup>
lred0080	2003 Aug 30.38623	2452881.886232	300	23.865 <sup>g</sup>
lred0081	2003 Aug 30.39075	2452881.890758	300	23.896 <sup>g</sup>
lred0114	2003 Aug 30.49488	2452881.994882	300	22.945 <sup>g</sup>
lred0115	2003 Aug 30.49949	2452881.999492	300	22.980 <sup>g</sup>
lred0116	2003 Aug 30.50404	2452882.004046	300	23.013 <sup>g</sup>
lred0117	2003 Aug 30.50860	2452882.008606	300	23.010 <sup>g</sup>

<sup>a</sup>Image number.<sup>b</sup>Decimal Universal Date at the start of the integration.<sup>c</sup>Julian Date at the start of the integration. No light-time correction has been made in the table.<sup>d</sup>Exposure time for the image.<sup>e</sup>Apparent red magnitude, uncertainties are  $\pm 0.02$ .<sup>f</sup>The apparent magnitude is for the V-band, uncertainties are  $\pm 0.03$ <sup>g</sup>The apparent magnitude is for the B-band, uncertainties are  $\pm 0.04$ . In the B-band, only light longward of 0.460  $\mu\text{m}$  was observed because of the dichroic.

TABLE 4. Large Objects With Extreme Light Curves<sup>a</sup>

Name	Type	$a \times b$ (km)	$\Delta$ mag (mag)	Period (hrs)	Cause <sup>b</sup>	Ref <sup>c</sup>
Iapetus	Saturn Satellite	$715 \times 715$	2	1903.9	AL	1
624 Hektor	Jupiter Trojan	$150 \times 75$	1.1	6.921	CB	2
216 Kleopatra	Main-Belt Asteroid	$109 \times 47$	1.18	5.385	JE/CB	3
2001 QG <sub>298</sub>	Kuiper Belt Object	$267 \times 94$	1.14	13.7744	CB	This Work

<sup>a</sup>Objects that have effective radii  $> 25$  km and lightcurves with peak-to-peak amplitudes  $> 1$  magnitudes.

<sup>b</sup>The dominant cause or most probable dominant cause for the amplitude of the lightcurve: AL is albedo, CB is contact binary, JE is Jacobi triaxial rotational ellipsoid

<sup>c</sup>References for specified objects: 1) Millis (1977) 2) Dunlap & Gehrels (1969); Hartmann & Cruikshank (1978); Weidenschilling (1980); Leone et al. (1984); Lagerkvist, Harris & Zappala (1989) 3) Scaltriti & Zappala (1978); Tholen (1980); Leone et al. (1984); Lagerkvist, Harris & Zappala (1989); Ostro et al. (2000); Hestroffer et al. (2002); Washabaugh & Scheeres (2002)

TABLE 5. Possible Contact Binaries in the Kuiper Belt

Name	$H^a$ (mag)	$\Delta m_R^b$ (mag)	Period <sup>c</sup> (hrs)	Probability <sup>d</sup>	Ref <sup>e</sup>
2001 QG <sub>298</sub>	6.85	$1.14 \pm 0.04$	$13.7744 \pm 0.0004$	very high	This Work
2000 GN <sub>171</sub>	5.98	$0.61 \pm 0.03$	$8.329 \pm 0.005$	high	1
(33128) 1998 BU <sub>48</sub>	7.2	$0.68 \pm 0.04$	$9.8 \pm 0.1$	high	1
(26308) 1998 SM <sub>165</sub>	5.8	$0.45 \pm 0.03$	$7.1 \pm 0.1$	medium	1,2
(32929) 1995 QY <sub>9</sub>	7.5	$0.60 \pm 0.04$	$7.3 \pm 0.1$	medium	1
(20000) Varuna 2000 WR <sub>106</sub>	3.21	$0.42 \pm 0.03$	$6.34 \pm 0.01$	low	3

<sup>a</sup>Absolute magnitude.

<sup>b</sup>The peak to peak range of the lightcurve.

<sup>c</sup>The lightcurve period if there is two maximum per period.

<sup>d</sup>Probability that the object is a contact or nearly contact binary.

<sup>e</sup>References for lightcurve information: 1) Sheppard & Jewitt (2002) 2) Romanishin et al. (2001) 3) Jewitt & Sheppard (2002)